International Journal of Heat and Mass Transfer 221 (2024) 125038

Contents lists available at ScienceDirect

International Journal of Heat and Mass Transfer

journal homepage: www.elsevier.com/locate/ijhmt

Thermal stability of a two-dimensional multilayer diffusion-reaction problem

Ankur Jain*, Girish Krishnan

Mechanical and Aerospace Engineering Department, University of Texas at Arlington, Arlington, TX, USA

ARTICLE INFO

Keywords:
Diffusion-reaction problems
Multilayer transport
Stability analysis
Li-ion cells

ABSTRACT

Multilayer diffusion-reaction problems appear commonly in heat and mass transfer analysis, including in thermal management of Li-ion batteries, drug delivery and reacting systems. Thermal stability of diffusion-reaction problems is of much interest due to the potential for thermal runaway in such systems. While there is some past work on investigating thermal instability in a one-dimensional multilayer body, practical systems such as Li-ion cells are often two- or even three-dimensional. Therefore, it is important to develop a theoretical understanding of when a two-dimensional multilayer diffusion-reaction system may be thermally unstable. This work addresses this important question by deriving a solution for the transient temperature field in this problem, followed by pole analysis in the Laplace domain. An explicit threshold for thermal stability of the system is determined on the basis of the determinants associated with a set of algebraic equations. The impact of key non-dimensional numbers on thermal stability is determined, including those associated with heat generation and boundary cooling, as well as ratios of thermal properties of the layers. Good agreement with past papers for special cases of the general problem considered here is shown. A stability curve that separates stable and unstable regions in the thermal design space of a two-dimensional two-layered body, such as a stack of Li-ion cells is presented. This work extends the state-of-the-art in the theoretical understanding of thermal stability, and may also contribute towards design for safety of practical engineering systems.

1. Introduction

Theoretical analysis of simultaneous diffusion and linear reaction within a body is of much interest due to several scientific and engineering applications [1–3]. For example, in a multilayered Li-ion cell, temperature-dependent heat generation occurs due to decomposition reactions in each layer. Similarly, in a drug delivery device such as a capsule, diffusion of the active drug through the inactive polymer matrix is accompanied by drug absorption within the matrix, which is often modeled as a negative concentration-dependent reaction term [4,5]. Other problems where diffusion and reaction both occur include combustion [6], nuclear reactors [7], ecology [8] and geology [9].

Multilayer diffusion-reaction thermal problems are of particular interest in studying thermal runaway in Li-ion batteries [2,10,11]. Thermal runaway refers to a series of exothermic decomposition reactions, wherein heat generated in the reactions increases the cell temperature, which further increases the heat generated, due to a positive rate of change of the reaction rate with temperature, until an unsustainable rate of temperature rise results in fire and explosion [12,13]. Transient thermal conduction in such a scenario is an eigenvalue problem involving diffusion and reaction, for which, the transient temperature distribution may be written in an infinite series form [2,10]. As is the usual case with this technique, the eigenvalues of the problem are determined using the associated boundary and interface conditions [2,10,14,15]. Under certain conditions, it has been shown [2,10,15] that such problems may admit one or more imaginary eigenvalues, which have been shown to directly correspond to instability and thermal runaway [2,10,15]. Based on this, conditions for thermal stability of such systems have been derived [2,10,15].

A key drawback of the technique summarized above is that deriving exact explicit expressions for the temperature distribution and the stability criterion is often cumbersome, especially for more than a few layers. Since the primary interest is often in determining whether a given system is stable or not, and not necessarily in computing the temperature distribution itself, therefore, alternate methods to determine the thermal stability of diffusion-reaction systems are of interest. For example, linear stability theory predicts that, in general, a function diverges at large times when its Laplace transform has at least one pole with a positive real component [16]. Based on this, the thermal stability

* Corresponding author.
E-mail address: jaina@uta.edu (A. Jain).

https://doi.org/10.1016/j.ijheatmasstransfer.2023.125038
Received 10 August 2023; Received in revised form 24 November 2023; Accepted 3 December 2023
Available online 27 December 2023

Nomenclature

A, B, C, D	coefficients
Bi	Biot number
k	thermal conductivity ($Wm^{-1}K^{-1}$)
$\bar{k}$	non-dimensional thermal conductivity
L	layer thickness (m)
T	temperature (K)
s	Laplace variable (s^{-1})
t	time (s)
$\bar{t}$	non-dimensional time (s)
w	width (m)
$\bar{w}$	non-dimensional width
$x,\ y$	spatial coordinates (m)
$\bar{x},\ \bar{y}$	non-dimensional spatial coordinates (m)
α	diffusivity (m^2s^{-1})
$\bar{\alpha}$	non-dimensional diffusivity
β	heat generation coefficient (s^{-1})
$\bar{\beta}$	non-dimensional heat generation coefficient
Δ	determinant
θ	non-dimensional temperature
σ	non-dimensional interface location
λ	eigenvalue

Subscripts

1,2	layer number
amb	ambient
in	initial value

of a one-dimensional multilayer diffusion-reaction problem has been investigated by examining the poles of the solution in the Laplace domain [3]. Stability of such a system is governed by a balance between heat dissipation through diffusion and heat generation due to reaction. Another work used similar pole analysis to examine the stability of a temperature-dependent heat-generating finite body surrounded by a semi-infinite medium [17]. Such an approach provides a straightforward technique to determine if, for a given set of parameter values, the problem is stable or not. Despite the papers cited above, however, there remains a lack of sufficient work on using linear stability theory to investigate thermal problems.

Further, most of the past work in thermal stability of multilayer diffusion-reaction systems addresses one-dimensional systems [2,3,10,11,14,17]. While the one-dimensional approximation is reasonable for several practical engineering systems, multidimensional analysis may be necessary for specific problems. For example, thermal transport in a battery pack containing a number of closely-packed prismatic Li-ion cells is inherently two-dimensional – conduction from one cell to the other in the thickness direction, as well as heat spreading within each cell are both important. Multidimensional analysis is clearly necessary to compute the temperature distribution and determine the stability of such systems. Unfortunately, one-dimensional models cannot be readily extended to analyze multidimensional problems, where the boundary conditions in the direction normal to the layered direction may become important, making such problems a lot more complicated than one-dimensional problems.

The relatively small amount of literature on analytical modeling of multi-dimensional thermal conduction problems is limited only to isothermal (very large Biot number) or adiabatic (zero Biot number) boundary conditions along the sidewalls [15,18–21]. This assumption has been made in the literature mainly to enable a single set of eigenvalues for all layers, which makes it easy to satisfy interface conditions. This strategy, however, breaks down for the realistic scenario of a convective boundary condition along the sidewalls, because each layer must now have a distinct set of eigenvalues. Recent work on a two-dimensional two-layer problem generalized this to include a general convective boundary condition, but did not account for the reaction term [14] that is mainly responsible for thermal instability. Clearly, there remains a need to examine the stability of two-dimensional multilayer diffusion-reaction problems under general convective boundary conditions, so as to be relevant for practical applications where the sidewalls are neither isothermal nor adiabatic.

This work addresses this gap in the literature by carrying out Laplace transform based stability analysis of a two-dimensional multilayered diffusion-reaction problem, where each layer has a general convective boundary condition normal to the layered direction. The problem is solved in the Laplace domain, the inversion of which provides the transient temperature field. Moreover, the poles of the temperature field in the Laplace domain are examined, leading to a closed-form stability threshold involving the determinants associated with a set of linear algebraic equations. It is shown that this method correctly predicts the threshold between thermal instability and stability of the system. Good agreement with past work for two specific special cases is also demonstrated. The impact of non-dimensional numbers associated with temperature-dependent heat generation and boundary cooling on thermal stability is examined.

The next Section defines and non-dimensionalizes the problem. A solution of the problem is presented in Section 3, followed by stability analysis in Section 4. Key results are discussed in Section 5.

2. Problem definition and non-dimensionalization

The primary interest of the present work is to determine the stability of the linear diffusion-reaction heat transfer problem in a two-dimensional multilayer body. For simplicity, a two-layer body is considered, as shown schematically in Fig. 1, although results are easily extendable to more than two layers. The thicknesses of the two bodies are L_1 and L_2, respectively, with a width $2w$ of each layer. Thermal conductivity and diffusivity of each layer are denoted by k and α, respectively. Perfect thermal contact between the two layers is assumed. The ambient temperature is taken to be T_{amb}, and a uniform initial temperature T_{in} is assumed for each layer.

Temperature-dependent heat generation within each layer may occur due to a variety of mechanisms, such as chemical reactions and Joule heating. While such heat generation mechanisms may, in general, be non-linearly temperature dependent, for example due to exponential Arrhenius kinetics for chemical reactions [22], linearization is often carried out as an approximation, i.e., heat generation is assumed to exhibit a linear temperature dependence [2,11].

The sidewalls of each layer are assumed to be subjected to a general convective boundary condition represented by convective heat transfer coefficients h_1 and h_2, respectively. Note that setting these coefficients to zero produces the special case of adiabatic wall, while assuming a very large value results in an isothermal wall. Similar to the sidewalls, general convective conditions may also exist on the top and bottom walls at the ends of the geometry shown in Fig. 1. Since the effect of boundary conditions at the ends of the multilayer geometry have been extensively investigated in past work on one-dimensional multilayer stability analysis [2,10], therefore, the focus of the present work is on the effect of sidewall boundary conditions, which occurs primarily due to the two-dimensional nature of the problem considered here. For simplification, therefore, the top and bottom boundaries are assumed to be isothermal, as shown in Fig. 1. This assumption may also align well with common practical systems, in which, a cold plate or a boiling coolant may maintain constant temperature at the two ends of the multilayer body. Generalization of the problem to include convective boundary

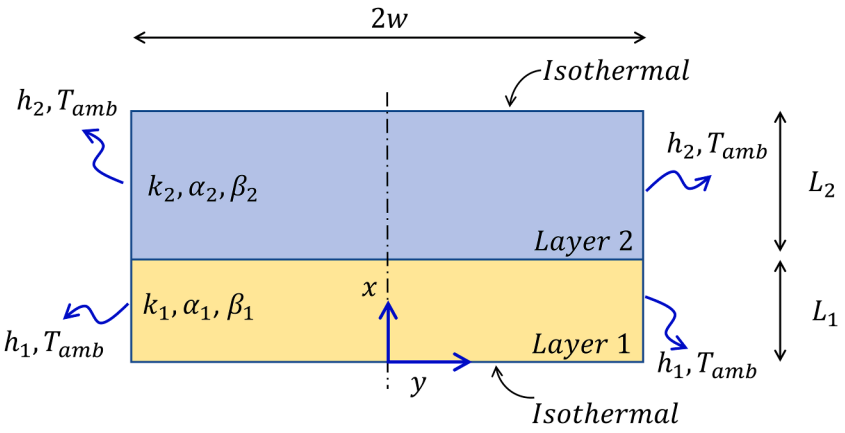

Fig. 1. Schematic of the two-dimensional two-layer diffusion-reaction problem considered in this work.

conditions at the top and bottom is briefly discussed in a later sub-section.

Based on symmetry of the problem in the y-direction, only one half of the problem $0 < y < w$ may be considered. Under these assumptions, temperature field in the two layers, $T_i(x,t)$ $(i=1,2)$ is governed by the following differential equations based on the principle of energy conservation:

$$\alpha_i\left(\frac{\partial^2 T_i}{\partial x^2}+\frac{\partial^2 T_i}{\partial y^2}\right)+\beta_i(T_i-T_{amb})=\frac{\partial T_i}{\partial t}\ (i=1,2) \tag{1}$$

where β_i is the linear coefficient that represents the temperature-dependence of heat generation [2,10]. The larger the value of β_i, the more aggressively does heat generation increase with temperature. Note that Eq. (1) is valid in the range $0 < y < w$ in the y-direction, and in the range $0 < x < L_1$ for layer 1 and $L_1 < x < L_1 + L_2$ for layer 2 in the x-direction.

The associated boundary conditions are

$$\frac{\partial T_i}{\partial y}=0\ (y=0)\ (i=1,2) \tag{2}$$

$$k_i\frac{\partial T_i}{\partial y}+h_i(T_i-T_{amb})=0\ (y=w)\ (i=1,2) \tag{3}$$

$$T_1=T_{amb}\ (x=0) \tag{4}$$

$$T_2=T_{amb}\ (x=L_1+L_2) \tag{5}$$

Note that Eq. (2) arises from symmetry in the problem, as shown in Fig. 1. Eqs. (3)–(5) represent the convective and isothermal boundary conditions assumed at the sidewall and top/bottom boundaries, respectively, as shown in Fig. 1.

Based on perfect thermal contact between layers, the following interface conditions may be written:

$$T_1=T_2\ \ (x=L_1) \tag{6}$$

$$k_1\frac{\partial T_1}{\partial y}=k_2\frac{\partial T_2}{\partial y}\ (x=L_1) \tag{7}$$

Finally, the initial condition may be expressed simply as

$$T_i=T_{in}\ (t=0)\ (i=1,2) \tag{8}$$

In order to solve the problem described above and to examine the stability of the temperature field, non-dimensionalization is first carried out, based on the following definitions of non-dimensional parameters

$$\theta_i=\frac{(T_i-T_{amb})}{T_{in}-T_{amb}};\ \bar{x}=\frac{x}{L_1+L_2};\ \bar{y}=\frac{y}{L_1+L_2};\ \bar{t}=\frac{\alpha_2 t}{(L_1+L_2)^2};\ \sigma=\frac{L_1}{L_1+L_2};\ \bar{w}=\frac{w}{L_1+L_2};\ \bar{k}_1=\frac{k_1}{k_2};\ \bar{\alpha}_1=\frac{\alpha_1}{\alpha_2};\ Bi_i=\frac{h_i(L_1+L_2)}{k_2};\ \bar{\beta}_i=\frac{\beta_i(L_1+L_2)^2}{\alpha_2} \tag{9}$$

Here, $\bar{x}$, $\bar{y}$ and $\bar{t}$ are the non-dimensional coordinates, θ_i are the non-dimensional temperature fields in each layer ($i = 1,\ 2$), σ is the non-dimensional location of the interface, $\bar{w}$ is the non-dimensional half-width, Bi_i $(i=1,\ 2)$ are the Biot numbers at the sidewalls of each layer, and $\bar{\beta}_i$ $(i=1,\ 2)$ are the non-dimensional heat generation coefficients in each layer. In general, thermal stability of this problem is determined by a balance between thermal transport within and between layers (represented by $\bar{\alpha}_1$ and $\bar{k}_1$), heat removal from the boundaries (Bi_1 and Bi_2) and heat generation within each layer ($\bar{\beta}_1$ and $\bar{\beta}_2$). Non-dimensionalization based on Eq. (9) reduces the number of parameters involved in the problem and helps identify key non-dimensional parameters that govern the thermal stability of the problem.

In addition to non-dimensionalization, Laplace transformation of the governing equations is also carried out in order to remove time dependence from the equations. The following set of non-dimensional governing equations in the Laplace domain is obtained:

$$\bar{\alpha}_1\left(\frac{\partial^2\widehat{\theta}_1}{\partial\bar{x}^2}+\frac{\partial^2\widehat{\theta}_1}{\partial\bar{y}^2}\right)+\bar{\beta}_1\widehat{\theta}_1=s\widehat{\theta}_1-1 \tag{10}$$

$$\frac{\partial^2\widehat{\theta}_2}{\partial\bar{x}^2}+\frac{\partial^2\widehat{\theta}_2}{\partial\bar{y}^2}+\bar{\beta}_2\widehat{\theta}_2=s\widehat{\theta}_2-1 \tag{11}$$

subject to

$$\frac{\partial\widehat{\theta}_i}{\partial\bar{y}}=0\ (\bar{y}=0)\ (i=1,2) \tag{12}$$

$$\bar{k}_1\frac{\partial\widehat{\theta}_1}{\partial\bar{y}}+Bi_1\widehat{\theta}_1=0\ (\bar{y}=\bar{w}) \tag{13}$$

$$\frac{\partial\widehat{\theta}_2}{\partial\bar{y}} + Bi_2\widehat{\theta}_2 = 0 \ (\bar{y}=\bar{w}) \tag{14}$$

$$\widehat{\theta}_1 = 0 \ (\bar{x}=0) \tag{15}$$

$$\widehat{\theta}_2 = 0 \ (\bar{x}=1) \tag{16}$$

$$\widehat{\theta}_1 = \widehat{\theta}_2 \ (\bar{x}=\sigma) \tag{17}$$

$$\bar{k}_1\frac{\partial\widehat{\theta}_1}{\partial\bar{x}} = \frac{\partial\widehat{\theta}_2}{\partial\bar{x}} \ (\bar{x}=\sigma) \tag{18}$$

Where ^ represents quantities in the Laplace domain.

3. Derivation of the solution

The problem for the non-dimensional temperature field in the Laplace domain is solved using the method of separation of variables. First, in order to account for the non-homogeneity appearing in Eqs. (10) and (11), the following transformation is carried out

$$\widehat{\theta}_i(\bar{x},\bar{y}) = \widehat{u}_i(\bar{y}) + \widehat{v}_i(\bar{x},\bar{y}) \ (i=1,2) \tag{19}$$

where the dependence on the Laplace variable s is not listed explicitly for convenience.

$\widehat{u}_1$ and $\widehat{u}_2$ may be taken to be governed by $\bar{\alpha}_1\widehat{u}_1^{''} + (\bar{\beta}_1 - s)\widehat{u}_1 = -1$ and $\widehat{u}_2^{''} + (\bar{\beta}_2 - s)\widehat{u}_2 = -1$, respectively. The associated boundary/interface conditions are $\widehat{u}_1^{'} = \widehat{u}_2^{'} = 0$ at $\bar{y}=0$, $\bar{k}_1\widehat{u}_1^{'} + Bi_1\widehat{u}_1 = 0$ at $\bar{y}=\bar{w}$ and $\widehat{u}_2^{'} + Bi_2\widehat{u}_2 = 0$ at $\bar{y}=\bar{w}$. A solution for this set of ordinary differential equations is found to be

$$\widehat{u}_i(\bar{y}) = (s-\bar{\beta}_i)^{-1} + A_i\cos(\mu_i\bar{y}) \ (i=1,2) \tag{20}$$

where $\mu_1 = \sqrt{(\bar{\beta}_1 - s)/\bar{\alpha}_1}$ and $\mu_2 = \sqrt{\bar{\beta}_2 - s}$. Based on the boundary conditions at $\bar{y}=\bar{w}$, the coefficients A_i are found to be $A_1 = -\frac{Bi_1}{s-\bar{\beta}_1}(Bi_1\cos(\mu_1\bar{w}) - \bar{k}_1\mu_1\sin(\mu_1\bar{w}))^{-1}$ and $A_2 = -\frac{Bi_2}{s-\bar{\beta}_2}(Bi_2\cos(\mu_2\bar{w}) - \mu_2\sin(\mu_2\bar{w}))^{-1}$. Note that when $s=\bar{\beta}_1$, $\widehat{u}_1(\bar{y})$ is given by the following expression instead of Eq. (20)

$$\widehat{u}_1(\bar{y}) = \frac{1}{\bar{\alpha}_1}\left(\frac{-\bar{y}^2}{2} + \frac{\bar{k}_1\bar{w}}{Bi_1} + \frac{\bar{w}^2}{2}\right) \tag{21}$$

Similarly, when $s=\bar{\beta}_2$, $\widehat{u}_2(\bar{y})$ is given by the following expression instead of Eq. (20)

$$\widehat{u}_2(\bar{y}) = \frac{-\bar{y}^2}{2} + \frac{\bar{w}}{Bi_2} + \frac{\bar{w}^2}{2} \tag{22}$$

$\widehat{v}_i(\bar{x},\bar{y})$ are determined next. Based on the definition of $\widehat{u}_i$, the governing equations for $\widehat{v}_i(\bar{x},\bar{y})$ are given by

$$\bar{\alpha}_1\left(\frac{\partial^2\widehat{v}_1}{\partial\bar{x}^2} + \frac{\partial^2\widehat{v}_1}{\partial\bar{y}^2}\right) + \bar{\beta}_1\widehat{v}_1 = s\widehat{v}_1 \tag{23}$$

$$\frac{\partial^2\widehat{v}_2}{\partial\bar{x}^2} + \frac{\partial^2\widehat{v}_2}{\partial\bar{y}^2} + \bar{\beta}_2\widehat{v}_2 = s\widehat{v}_2 \tag{24}$$

subject to

$$\frac{\partial\widehat{v}_i}{\partial\bar{y}} = 0 \ (\bar{y}=0) \ (i=1,2) \tag{25}$$

$$\bar{k}_1\frac{\partial\widehat{v}_1}{\partial\bar{y}} + Bi_1\widehat{v}_1 = 0 \ (\bar{y}=\bar{w}) \tag{26}$$

$$\frac{\partial\widehat{v}_2}{\partial\bar{y}} + Bi_2\widehat{v}_2 = 0 \ (\bar{y}=\bar{w}) \tag{27}$$

$$\widehat{v}_1 = -\widehat{u}_1(\bar{y}) \ (\bar{x}=0) \tag{28}$$

$$\widehat{v}_2 = -\widehat{u}_2(\bar{y}) \ (\bar{x}=1) \tag{29}$$

$$\widehat{v}_1 = \widehat{v}_2 + (\widehat{u}_2(\bar{y}) - \widehat{u}_1(\bar{y})) \ (\bar{x}=\sigma) \tag{30}$$

$$\bar{k}_1\frac{\partial\widehat{v}_1}{\partial\bar{x}} = \frac{\partial\widehat{v}_2}{\partial\bar{x}} \ (\bar{x}=\sigma) \tag{31}$$

The following series solution may be written for $\widehat{v}_1$ and $\widehat{v}_2$:

$$\widehat{v}_1(\bar{x},\bar{y}) = \sum_{n=1}^{\infty}\left[C_{1,n}\cosh\left(\eta_{1,n}\bar{x}\right) + D_{1,n}\sinh\left(\eta_{1,n}\bar{x}\right)\right]\cos\left(\lambda_{1,n}\bar{y}\right) \tag{32}$$

$$\widehat{v}_2(\bar{x},\bar{y}) = \sum_{n=1}^{\infty}\left[C_{2,n}\cosh\left(\eta_{2,n}(1-\bar{x})\right) + D_{2,n}\sinh\left(\eta_{2,n}(1-\bar{x})\right)\right]\cos\left(\lambda_{2,n}\bar{y}\right) \tag{33}$$

where $\lambda_{1,n}$ and $\lambda_{2,n}$ are the eigenvalues for the respective layers. Based on the governing equations, it can be shown that $\eta_{1,n} = \sqrt{\lambda_{1,n}^2 - (\bar{\beta}_1 - s)/\bar{\alpha}_1}$ and $\eta_{2,n} = \sqrt{\lambda_{2,n}^2 - (\bar{\beta}_2 - s)}$. Further, based on the boundary condition at $\bar{y}=\bar{w}$, the following eigenequations may be derived for layers 1 and 2, respectively:

$$-\bar{k}_1 x\cdot\tan(x\bar{w}) + Bi_1 = 0 \tag{34}$$

$$-x\cdot\tan(x\bar{w}) + Bi_2 = 0 \tag{35}$$

Roots of the transcendental equations given by Eqs. (34) and (35) provide the eigenvalues $\lambda_{1,n}$ and $\lambda_{2,n}$, respectively, which are, in general, distinct from each other.

For practical computation, the infinite series solutions given by Eqs. (32) and (33) are truncated up to a finite number of terms, say, N, and a set of $4N$ linear algebraic equations in the $4N$ unknowns $C_{1,n}$, $C_{2,n}$, $D_{1,n}$ and $D_{2,n}$ ($n=1,2\ldots N$) are derived using boundary and interface conditions in the $\bar{x}$ direction. Boundary conditions at $\bar{x}=0$ and $\bar{x}=1$ result in

$$\sum_{n=1}^{\infty} C_{i,n}\cos\left(\lambda_{i,n}\bar{y}\right) = -\widehat{u}_i(\bar{y}) \ (i=1,2) \tag{36}$$

Multiplying both sides of Eq. (36) above by $\cos(\lambda_{i,m}\bar{y})$ ($m=1,2,..N$), followed by integration and use of the principle of orthogonality of the eigenfunctions results in the following explicit expressions for $C_{1,n}$ and $C_{2,n}$:

$$C_{i,n} = -\frac{1}{N_{i,n}}\int_0^{\bar{w}}\widehat{u}_i(\bar{y})\cos\left(\lambda_{i,n}\bar{y}\right)d\bar{y} \ \ (i=1,2) \ \ (n=1,2,..N) \tag{37}$$

where the norms $N_{1,n}$ and $N_{2,n}$ are given by

$$N_{i,n} = \int_0^{\bar{w}}\cos^2\left(\lambda_{i,n}\bar{y}\right)d\bar{y} \ \ (i=1,\ 2) \ \ (n=1,2,..N) \tag{38}$$

Unfortunately, similar explicit equations for the other set of coefficients, $D_{1,n}$ and $D_{2,n}$ can not be obtained. Instead, from the interface conditions at $\bar{x}=\sigma$, one may write

$$\sum_{n=1}^{N}\left[C_{1,n}\cosh\left(\eta_{1,n}\sigma\right)+D_{1,n}\sinh\left(\eta_{1,n}\sigma\right)\right]\cos\left(\lambda_{1,n}\bar{y}\right)=\widehat{u}_2(\bar{y})-\widehat{u}_1(\bar{y})+\sum_{n=1}^{\infty}\left[C_{2,n}\cosh\left(\eta_{2,n}(1-\sigma)\right)+D_{2,n}\sinh\left(\eta_{2,n}(1-\sigma)\right)\right]\cos\left(\lambda_{2,n}\bar{y}\right) \tag{39}$$

$$\bar{k}_1\sum_{n=1}^{N}\eta_{1,n}\left[C_{1,n}\sinh\left(\eta_{1,n}\sigma\right)+D_{1,n}\cosh\left(\eta_{1,n}\sigma\right)\right]\cos\left(\lambda_{1,n}\bar{y}\right)=-\sum_{n=1}^{\infty}\eta_{2,n}\left[C_{2,n}\sinh\left(\eta_{2,n}(1-\sigma)\right)+D_{2,n}\cosh\left(\eta_{2,n}(1-\sigma)\right)\right]\cos\left(\lambda_{2,n}\bar{y}\right) \tag{40}$$

where, based on Eq. (37), $C_{1,n}$ and $C_{2,n}$ are already known. In order to determine the remaining coefficients $D_{1,n}$ and $D_{2,n}$, Eq. (39) is multiplied by $\cos(\lambda_{2,m}\bar{y})$ $(m=1,2..N)$ and integrated over $\bar{y}$. Mathematical simplification based on orthogonality of eigenfunctions of layer 2 results in

$$-D_{2,m}\sinh\left(\eta_{2,m}(1-\sigma)\right)N_{2,m}+\sum_{n=1}^{N}D_{1,n}\sinh\left(\eta_{1,n}\sigma\right)\int_0^{\bar{w}}\cos\left(\lambda_{1,n}\bar{y}\right)\cos\left(\lambda_{2,m}\bar{y}\right)dy=-\sum_{n=1}^{N}C_{1,n}\cosh\left(\eta_{1,n}\sigma\right)\int_0^{\bar{w}}\cos\left(\lambda_{1,n}\bar{y}\right)\cos\left(\lambda_{2,m}\bar{y}\right)dy+C_{2,m}\cosh\left(\eta_{2,m}(1-\sigma)\right)N_{2,m}+\int_0^{\bar{w}}\left[\widehat{u}_2(\bar{y})-\widehat{u}_1(\bar{y})\right]\cos\left(\lambda_{2,m}\bar{y}\right)dy \tag{41}$$

Eq. (41) represents N linear algebraic equations for each $m=1,2..N$.

Further, Eq. (40) is multiplied by $\cos(\lambda_{1,m}\bar{y})$ $(m=1,2..N)$ and integrated over $\bar{y}$. Mathematical simplification based on orthogonality of eigenfunctions of layer 1 results in

$$\bar{k}_1\eta_{1,m}D_{1,m}\cosh\left(\eta_{1,m}\sigma\right)N_{1,m}+\sum_{n=1}^{N}\eta_{2,n}D_{2,n}\cosh\left(\eta_{2,n}(1-\sigma)\right)\int_0^{\bar{w}}\cos\left(\lambda_{1,m}\bar{y}\right)\cos\left(\lambda_{2,n}\bar{y}\right)dy=-\bar{k}_1\eta_{1,m}C_{1,m}\sinh\left(\eta_{1,m}\sigma\right)N_{1,m}-\sum_{n=1}^{N}\eta_{2,n}C_{2,n}\sinh\left(\eta_{2,n}(1-\sigma)\right)\int_0^{\bar{w}}\cos\left(\lambda_{1,m}\bar{y}\right)\cos\left(\lambda_{2,n}\bar{y}\right)dy \tag{42}$$

which represents an additional N linear algebraic equations for each $m=1,2..N$. Together, Eqs. (41) and (42) constitute $2N$ equations that can be solved to determine the $2N$ unknowns $D_{1,n}$ and $D_{2,n}$. Given that $C_{1,n}$ and $C_{2,n}$ are already known from Eq. (37), this completes the solution for $\widehat{v}_i$, and thus, the temperature distribution $\widehat{\theta}_i(\bar{x},\bar{y})$ in the two layers in the Laplace domain. Eqs. (41) and (42) are solved using matrix inversion. Due to the complicated nature of the temperature field in the Laplace domain, inversion to time domain is carried out numerically using de Hoog's algorithm [23–24]. As discussed next, inversion is not necessarily needed for stability analysis.

4. Stability analysis

Based on results from linear stability theory [16], thermal stability of the two-dimensional two-layer diffusion-reaction problem considered here is predicted by the nature of poles of the temperature distribution in the Laplace domain, $\widehat{\theta}_i$. A pole with a positive/negative real component indicates that the system is thermally unstable/stable, and a pole at $s=0$ may be used as a limiting condition for stability. In the present problem, since $\widehat{\theta}_i$ is the sum of two components $\widehat{u}_i$ and $\widehat{v}_i$, therefore it is important to examine the values of s at which a pole may appear for either $\widehat{u}_i$ or $\widehat{v}_i$, i.e., values at which $\widehat{u}_i$ or $\widehat{v}_i$ may become infinite. While from Eq. (20), $\widehat{u}_i$ may become infinite at certain values of s when $Bi_1\cos(\mu_1\bar{w})-\bar{k}_1\mu_1\sin(\mu_1\bar{w})=0$, Eq. (37) implies that $C_{i,n}$ will become $\mp\infty$ whenever $\widehat{u}_i$ becomes $\pm\infty$. Further, Eqs. (32) and (33) imply that this will lead to $\widehat{v}_i$ becoming $\mp\infty$, resulting in a finite value of the temperature distribution in Laplace domain, $\widehat{\theta}_i$. This is illustrated graphically in a later Section. Therefore, the poles of $\widehat{\theta}_i$ occur due to the $\widehat{v}_i$ – and not $\widehat{u}_i$ – component becoming infinite. This is illustrated graphically in the next section. Based on the definition of $\widehat{v}_i$ given by Eqs. (32) and (33), a pole for $\widehat{v}_i$ may occur when one or more of the coefficients $C_{i,n}$ and $D_{i,n}$ become infinite. From Eq. (37), $C_{i,n}$ are always bounded, and, therefore, the appearance of a pole for $\widehat{\theta}_i$ may ultimately be attributed to the coefficients $D_{i,n}$ becoming infinite. Since $D_{i,n}$ are coupled to each other through the set of linear algebraic Eqs. (41) and (42), therefore, from Cramer's rule [25], these coefficients are given by Δ_j/Δ, where Δ is the determinant of the matrix formed by the coefficients in Eqs. (41) and (42), and Δ_j is the determinant of the matrix formed by replacing the j^{th} column of the coefficient matrix with the column vector formed by the right hand side of Eqs. (41) and (42). This implies that the coefficients $D_{i,n}$ may become infinite, and hence a pole for $\widehat{v}_i$ may occur when the determinant Δ approaches zero, provided at least one of the determinants Δ_j remain non-zero. Finally, since the system is thermally unstable/stable if a positive/negative pole exists, therefore, a limiting condition of instability may be expressed as the determinant Δ of the algebraic equations given by Eqs. (41) and (42) at $s=0$ approaching zero, while at least one of the determinants Δ_j remains non-zero.

In general, the determinant is a function of a number of non-dimensional parameters that represent various competing thermal processes in this problem, for example, transport as represented by $\bar{k}_1$ and $\bar{\alpha}_1$, reaction as represented by $\bar{\beta}_1$ and $\bar{\beta}_2$, boundary dissipation as represented by Bi_1 and Bi_2, as well as geometry as represented by $\bar{w}$ and σ. For a given set of conditions, the determinant can be computed to determine the threshold between thermal stability and instability (while also verifying that at least one of the determinants Δ_j remains non-zero), and to address other design questions that are directly related to thermal

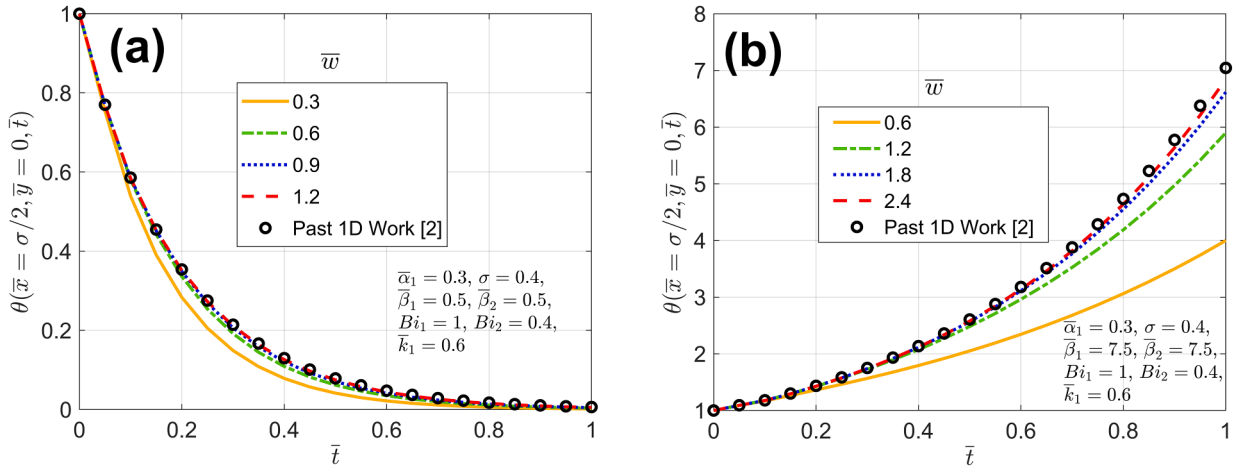

Fig. 2. Comparison with past work: Temperature at $\bar{x} = \sigma/2,\ \bar{y} = 0$ as a function of time for four different values of width $\bar{w}$. (a) and (b) illustrate thermally stable ($\bar{\beta}_1 = \bar{\beta}_2 = 0.5$) and unstable ($\bar{\beta}_1 = \bar{\beta}_2 = 7.5$) cases, respectively. Other problem parameters are $\bar{k}_1 = 0.6$, $\bar{\alpha}_1 = 0.3$, $\sigma = 0.4$, $Bi_1 = 1$, $Bi_2 = 0.4$. Results from past work on one-dimensional stability analysis [2] are presented for comparison.

safety. For example, in order to determine the maximum heat load $\bar{\beta}_1$ that the system can withstand before instability sets in, it suffices to determine the smallest $\bar{\beta}_1$ at which the determinant of Eqs. (41) and (42) at $s = 0$ approaches zero, while at least one of the determinants Δ_j remains non-zero. The role of the determinant in thermal stability of this problem is examined in more detail in analysis presented in the next section.

5. Results and discussion

5.1. Comparison with past work

The present work generalizes the analysis of multilayer thermal transport by accounting for two-dimensionality as well as the reaction term. Therefore, it is instructive to compare the present work with past results for special cases of the general problem considered here.

The two-dimensional two-layer problem considered here is expected to reduce to a simpler, one-dimensional problem when the width $\bar{w}$ becomes sufficiently large, which makes heat transfer in the $\bar{y}$ direction negligible. The one-dimensional multilayer diffusion-reaction problem has been solved in the past [2], for which, a limiting condition for stability was derived using separation of variables technique, independent of the pole analysis used in the present work. In order to compare the two, Fig. 2 presents the temperature distribution at a point in layer 1 ($\bar{x} = \sigma/2,\ \bar{y} = 0$) as a function of time. Two distinct problems with $\bar{\beta}_1 = \bar{\beta}_2 = 0.5$ and $\bar{\beta}_1 = \bar{\beta}_2 = 7.5$ that lead to convergence and divergence, respectively, are considered in Fig. 2(a) and 2(b), respectively. Other problem parameters are $\bar{k}_1 = 0.6$, $\bar{\alpha}_1 = 0.3$, $\sigma = 0.4$, $Bi_1 = 1$, $Bi_2 = 0.4$. Curves corresponding to multiple values of $\bar{w}$ are presented. For comparison, results from the one-dimensional multilayer diffusion-reaction analysis [2] are also presented in each case. It is found that as $\bar{w}$ increases, the temperature plot approaches the one obtained from an independent analysis of the limiting one-dimensional problem based on the separation of variables method [2]. For $\bar{w} = 1.2$ and $\bar{w} = 2.4$ in the converging and diverging cases, respectively, it is found that the two-dimensional analysis practically overlaps with the one-dimensional analysis, i.e., the width is large enough that the body can be treated as one-dimensional with reasonable accuracy. This limit, of course, depends on the values of other parameters that appear in the problem. For example, for larger values of Bi_1 and Bi_2, convective heat loss from the sidewalls is expected to be larger, and, therefore, the value

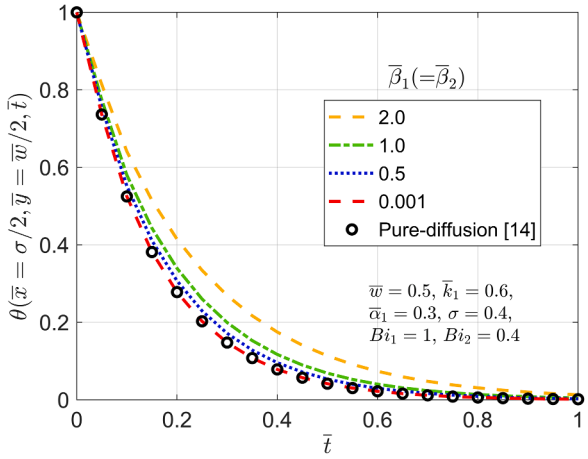

Fig. 3. Comparison with past work: Temperature at $\bar{x} = \sigma/2,\ \bar{y} = \bar{w}/2$ as a function of time for four different values of $\bar{\beta}_1 (= \bar{\beta}_2)$. Other problem parameters are $\bar{k}_1 = 0.6$, $\bar{\alpha}_1 = 0.3$, $\bar{w} = 0.5$, $\sigma = 0.4$, $Bi_1 = 1$, $Bi_2 = 0.4$. Results from past work on two-dimensional pure-diffusion analysis [14] are presented for comparison.

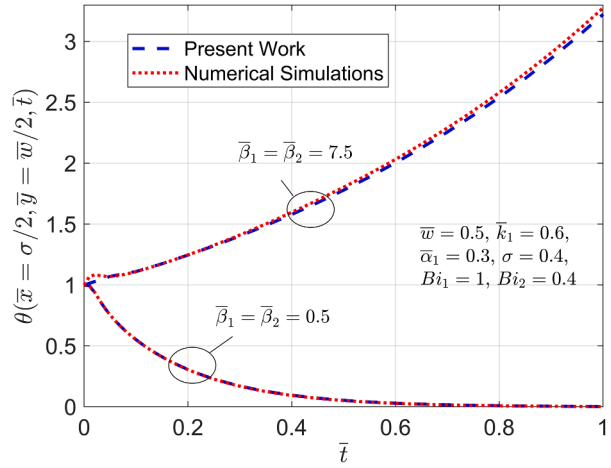

Fig. 4. Comparison with numerical simulations: Temperature at $\bar{x} = \sigma/2,\ \bar{y} = \bar{w}/2$ as a function of time for thermally stable ($\bar{\beta}_1 = \bar{\beta}_2 = 0.5$) and unstable ($\bar{\beta}_1 = \bar{\beta}_2 = 7.5$) cases. Other problem parameters are $\bar{k}_1 = 0.6$, $\bar{\alpha}_1 = 0.3$, $\bar{w} = 0.5$, $\sigma = 0.4$, $Bi_1 = 1$, $Bi_2 = 0.4$. Results from an independent numerical simulation are also shown for comparison.

of $\bar{w}$ for two-dimensional heat flow to be negligible is expected to be larger.

A further comparison of the present work with past results is presented for the special case of a two-dimensional pure-diffusion problem. In this context, the solution of a pure-diffusion problem in a two-dimensional two-layer body has been derived using the Laplace transformation technique [14]. In comparison, the present work is more general, in that a linearly temperature-dependent reaction term representative of thermal runaway in batteries and other reacting systems has been accounted for. In order to compare the two, a two-dimensional two-layer problem is considered with $\bar{k}_1 = 0.6$, $\bar{\alpha}_1 = 0.3$, $\sigma = 0.4$, $Bi_1 = 1$, $Bi_2 = 0.4$, $\bar{w} = 0.5$. Fig. 3 presents plots of temperature at $\bar{x} = \sigma/2$, $\bar{y} = \bar{w}/2$ in layer 1 for multiple values of the heat-generation coefficient $\bar{\beta}_1 (= \bar{\beta}_2)$. For comparison, results based on past work on the two-dimensional pure-diffusion problem [14] are also presented. Note that the past work considered a general convective boundary condition at the top and bottom ends of the two-layer body. For comparison with the present work, very large values are assumed for the corresponding Biot numbers, in order to obtain an isothermal boundary condition, similar to the present work. Fig. 3 shows that the temperature curves shift upwards as $\bar{\beta}_1$ increases, which is expected due to increased magnitude of heat generation at larger values of $\bar{\beta}_1$. As expected, for very small values of $\bar{\beta}_1$, the temperature curve based on the present work agrees well with past work, which was derived independent of the present work.

The plots above demonstrate that under simplified special cases, the general theoretical model presented in this work correctly reduces to special cases considered in past papers [2,14]. Such agreement is encouraging and lends confidence to the present work.

5.2. Comparison with numerical simulations

Comparison of the present work with numerical simulations is also carried out. For this purpose, a numerical simulation of the thermal conduction problem considered here is set up in a finite-element solver. The reaction term is implemented in the form of a heat generation term that increases linearly with the magnitude of the local temperature rise. The spatial grid and timestep for the simulation are chosen to be small enough ($\Delta\xi = \Delta\eta = 0.01$ and $\Delta\tau = 0.01$, respectively) so as to rule out sensitivity of computed temperature distribution on these parameters, as well as to ensure numerical stability. Fig. 4 presents a comparison between the analytical model and numerical simulations in terms of temperature at a specific location as a function of time for two representative problems – a converging one ($\bar{\beta}_1 = \bar{\beta}_2 = 0.5$) and a diverging one ($\bar{\beta}_1 = \bar{\beta}_2 = 7.5$). Other problem parameters are $\bar{k}_1 = 0.6$, $\bar{\alpha}_1 = 0.3$, $\sigma = 0.4$, $Bi_1 = 1$, $Bi_2 = 0.4$, $\bar{w} = 0.5$. In both cases, there is excellent agreement between the analytical model and numerical simulations. Minor disagreement (less than 1.6%) is observed at large times for the diverging cases, which may be due to the rapidly diverging nature of the temperature field because of the large values of $\bar{\beta}_1$ and $\bar{\beta}_2$, which may have induced computational error in the numerical simulation.

5.3. Results for a typical set of parameters

In order to better understand the thermal stability of this problem, pole analysis of a representative problem is carried out next. Fig. 5(a) plots the Laplace transform of the temperature field at a specific location $\bar{x} = \sigma/2$, $\bar{y} = \bar{w}/2$ as a function of the Laplace variable s. Curves are presented for four different values of $\bar{\beta}_1$, while other problem parameters are held constant at $\bar{k}_1 = 0.6$, $\bar{\alpha}_1 = 0.3$, $\sigma = 0.4$, $Bi_1 = 1, Bi_2 = 0.4$, $\bar{w} = 0.5$, $\bar{\beta}_2 = 0.5$. Poles of each curve are marked by solid circles. Based on linear stability theory, this problem is expected to be unstable if this curve exhibits a positive pole. As expected, it is found that for sufficiently small values of $\bar{\beta}_1$, the curve has a negative pole. This implies thermal stability, which is mainly because diffusion/conduction ($\bar{\alpha}_1$ and $\bar{k}_1$) and heat removal from the boundaries (Bi_1 and Bi_2) are sufficiently strong to overcome the relatively small temperature-dependent heat generation ($\bar{\beta}_1$ and $\bar{\beta}_2$). As $\bar{\beta}_1$ increases, the pole shifts rightwards, i.e., the problem approaches instability, and for a threshold value of around $\bar{\beta}_1 = 8.9$, crosses over to the positive s axis, indicating the onset of instability. Poles for larger values of $\bar{\beta}_1$ are found to be positive. Fig. 5(a) demonstrates the capability of the theoretical model developed here to predict the conditions in which the two-dimensional two-layer diffusion-reaction problem may exhibit instability.

To further examine the instability of this problem, Fig. 5(b) plots temperature at a specific location $\bar{x} = \sigma/2$, $\bar{y} = \bar{w}/2$ as a function of time for the same five values of $\bar{\beta}_1$ considered in Fig. 5(a). The temperature field is determined by inverse Laplace transformation of the solution derived in the Laplace domain, using de Hoog's algorithm as discussed in Section 3. Fig. 5(b) shows, as expected, that for $\bar{\beta}_1 = 1.0$ and $\bar{\beta}_1 = 6.0$, for which, Fig. 5(a) shows a negative pole, the temperature distribution correspondingly decays over time. In contrast, when the pole of the Laplace curve shown in Fig. 5(a) is positive (for $\bar{\beta}_1 = 12.0$ and $\bar{\beta}_1 = 15.0$), Fig. 5(b) clearly shows divergence in the corresponding plot of temperature as a function of time. The threshold value of $\bar{\beta}_1$, at which, the thermal system changes from unstable to stable is expected to be somewhere close to $\bar{\beta}_1 = 8.9$, which is consistent with Fig. 5(a).

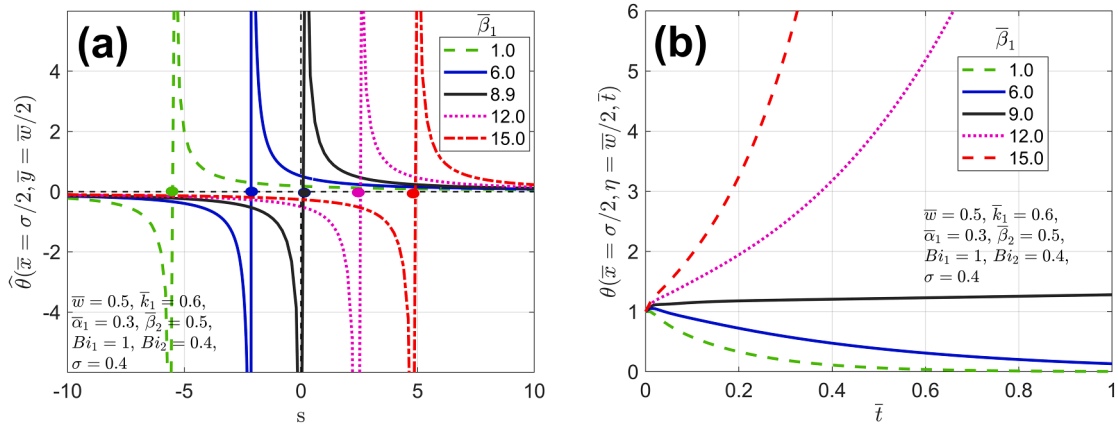

Fig. 5. (a) Temperature in the Laplace domain at $\bar{x} = \sigma/2$, $\bar{y} = \bar{w}/2$ as a function of the Laplace variable s. Curves are plotted for four different values of $\bar{\beta}_1$. Other problem parameters are $\bar{k}_1 = 0.6$, $\bar{\alpha}_1 = 0.3$, $\bar{\beta}_2 = 0.5$, $\bar{w} = 0.5$, $\sigma = 0.4$, $Bi_1 = 1$, $Bi_2 = 0.4$. (b) Temperature as a function of time at $\bar{x} = \sigma/2$, $\bar{y} = \bar{w}/2$ for the same values of $\bar{\beta}_1$ to illustrate stability/instability. $\bar{\beta}_1 = 8.9$ is found to be close to the threshold for stability.

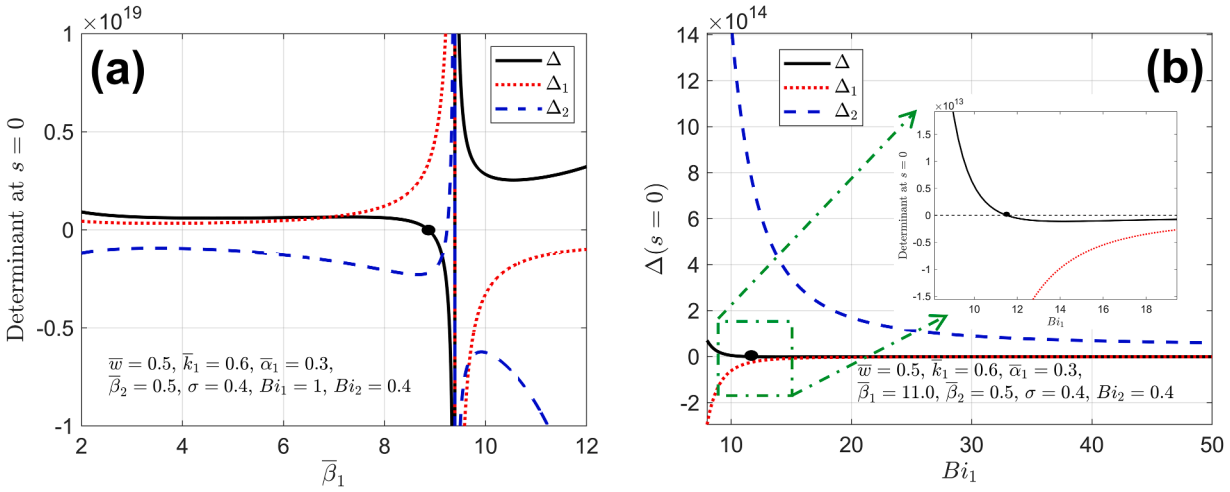

Fig. 6. Determinant as an indicator of stability: Determinants Δ, Δ_1 and Δ_2 associated with the linear algebraic equations given by Eqs. (41) and (42) at $s = 0$ as a function of (a) $\bar{\beta}_1$ (with $Bi_1 = 1$), (b) Bi_1 (with $\bar{\beta}_1 = 11.0$). Other problem parameters are $\bar{k}_1 = 0.6$, $\bar{\alpha}_1 = 0.3$, $\bar{\beta}_2 = 0.5$, $\bar{w} = 0.5$, $\sigma = 0.4$, $Bi_2 = 0.4$. A zoomed-in plot is also shown in (b) for clarity.

5.4. Determinant as an indicator of thermal stability

A key assertion of the present work is that the determinant of the set of algebraic equations for the coefficients of the series solution predicts the threshold between stability/instability of the problem. It is shown in Section 4 that a threshold for stability may be obtained by examining the values of various determinants associated with Eqs. (41) and (42) at $s = 0$. In order to demonstrate this further, Fig. 6 plots the magnitude of the determinant Δ at $s = 0$ for a representative problem. Since heat generation within the layers and heat removal from the boundaries are both important factors in determining the temperature distribution and thermal stability, therefore, the determinant Δ is plotted as a function of $\bar{\beta}_1$ and Bi_1 in Fig. 6(a) and 6(b), respectively, while all other problem parameters are held constant. As predicted by the theory presented in Section 4, the curve shown in Fig. 6(a) is found to cross the $\bar{\beta}_1$-axis, indicating a zero determinant at that point. This threshold value, found to be $\bar{\beta}_1 = 8.9$ from Fig. 6(a) is consistent with the pole analysis presented in Fig. 5(a), which shows that the pole of the curve for the Laplace transform of temperature just becomes positive for a threshold value of around $\bar{\beta}_1 = 8.9$. For values of $\bar{\beta}_1$ larger than this threshold, it is expected that temperature-dependent heat generation will dominate over dissipation processes, resulting in divergence of the temperature field at large times. Note that the determinant curve may cross the $\bar{\beta}_1$-axis multiple times. However, the first root is of primary interest, because, clearly, instability will occur for any value of $\bar{\beta}_1$ larger than the first root.

Note that in addition to Δ, Fig. 6(a) also plots two other associated determinants Δ_1 and Δ_2 formed by replacing the first and second columns, respectively, of the coefficient matrix with the column vector formed by the right hand side of Eqs. (41) and (42). These curves verify that the determinants Δ_1 and Δ_2 remain non-zero at $\bar{\beta}_1 = 8.9$, at which, Δ becomes zero. Based on the theoretical discussion in Section 4, this confirms that $\bar{\beta}_1 = 8.9$ is indeed the correct threshold for instability of this problem.

Fig. 6(b) presents a similar curve for the determinant as a function of Bi_1 that represents heat removal from the sidewall boundary. Similar to Fig. 6(a), the curve in Fig. 6(b) is also found to cross the Bi_1-axis at a specific value that represents the threshold value around $Bi_1 = 11.5$, below which, the boundary condition is not strong enough to prevent thermal instability. Similar to Fig. 6(a), the determinants Δ_1 and Δ_2 are also plotted here in addition to Δ, in order to correctly determine the threshold for instability. These curves help verify that the determinants Δ_1 and Δ_2 remain non-zero at $Bi_1 = 11.5$ when Δ becomes zero.

5.5. The origin of poles from $\hat{u}_i$ and $\hat{v}_i$ components

As shown in Eq. (19), the temperature distribution in the Laplace

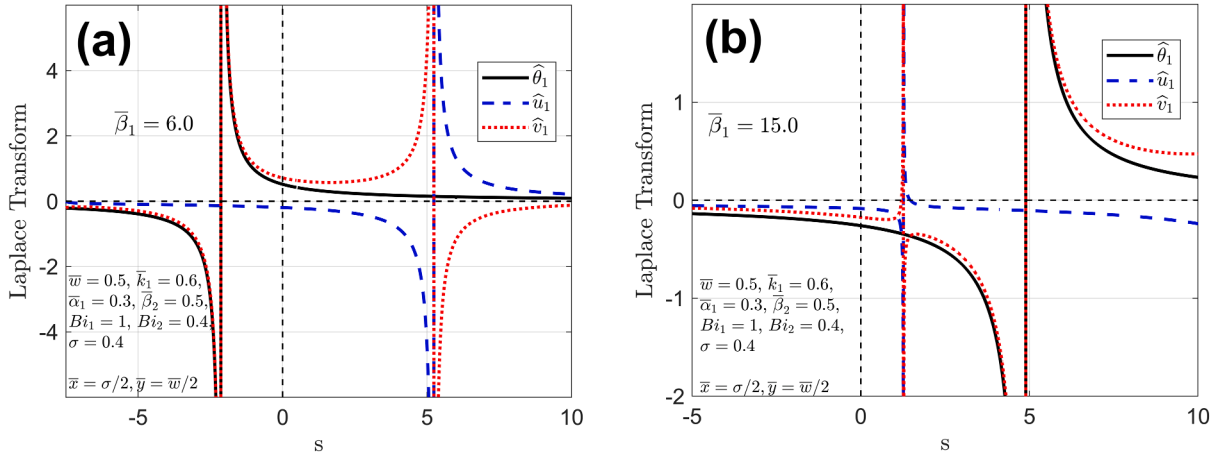

Fig. 7. Origin of poles from $\hat{v}_i$ component: $\hat{\theta}_1$ at $\bar{x} = \sigma/2$, $\bar{y} = \bar{w}/2$ as a function of the Laplace variable s, along with its two components $\hat{u}_1$ and $\hat{v}_1$. (a) $\bar{\beta}_1 = 6.0$, (b) $\bar{\beta}_1 = 15.0$. Other problem parameters are $\bar{k}_1 = 0.6$, $\bar{\alpha}_1 = 0.3$, $\bar{\beta}_2 = 0.5$, $\bar{w} = 0.5$, $\sigma = 0.4$, $Bi_1 = 1.0$, $Bi_2 = 0.4$.

domain comprises two components – $\widehat{u}_i(\bar{y})$ and $\widehat{v}_i(\bar{x},\bar{y})$. A key assertion presented in Section 4 is that the poles for the Laplace temperature distribution, which determine thermal stability of this problem, originate from the $\widehat{v}_i$ component, and not the $\widehat{u}_i$ component. Specifically, it is shown that poles occur due to the series coefficients $D_{i,n}$ becoming infinite when the determinant Δ of the algebraic equations given by Eqs. (41) and (42) at $s = 0$ approaches zero while at least one of the associated determinants Δ_j remain non-zero. In order to illustrate the origin of poles for the temperature distribution from the $\widehat{v}_i$ component, $\widehat{\theta}_1$ at a specific location $\bar{x} = \sigma/2,\ \bar{y} = \bar{w}/2$ is plotted as a function of the Laplace variable s, along with its two components $\widehat{u}_1$ and $\widehat{v}_1$ in Fig. 7. Two specific cases with $\bar{\beta}_1 = 6.0$ and $\bar{\beta}_1 = 15.0$ that represent thermally stable and thermally unstable conditions, respectively, are plotted in Fig. 7(a) and 7(b), respectively. In each case, within the range plotted, $\widehat{u}_1$ is found to exhibit one pole, at $s = 5.0$ and $s = 1.3$ for the two cases, respectively. However, as discussed in Section 4, due to the relationship between $\widehat{u}_1$ and $\widehat{v}_1$, $\widehat{v}_1$ is found to have an opposite pole at the same value of s, so that the sum $\widehat{\theta}_1$ does not exhibit a pole at that location. Therefore, Fig. 7(a) and 7(b) illustrate that for both stable and unstable problems, even though $\widehat{u}_1$ may have a pole, it does not lead to a pole for $\widehat{\theta}_1$, and, therefore plays no role in determining the stability of the problem. In contrast, both plots show that $\widehat{v}_1$ has a pole at $s = -1.9$ and $s = 5.0$ for the two cases, respectively, at which, the $\widehat{u}_1$ component remains finite, which leads to a pole for $\widehat{\theta}_1$ at these locations. The negative and positive values of s at these pole locations indicate thermal stability and instability for the parameter values in Fig. 7(a)(a) and 7(b), respectively. Fig. 7 illustrates that tracking the pole for $\widehat{v}_i$ is indeed appropriate for determining the poles of the overall temperature distribution in the Laplace domain, and, thus determining the thermal stability of the problem.

5.6. Convergence vs divergence: stability maps

A primary question of much practical importance is whether, for a given set of conditions, the temperature field in the two-dimensional two-layer body will converge or diverge. In general, thermal stability is governed by a balance between multiple competing processes, including heat generation (represented in non-dimensional form by $\bar{\beta}_1$ and $\bar{\beta}_2$), heat dissipation from the sidewalls (represented by Bi_1 and Bi_2), diffusion in the body (represented by $\bar{\alpha}_1$), interfacial heat transfer between layers (represented by $\bar{k}_1$) and geometry (represented by σ and $\bar{w}$).

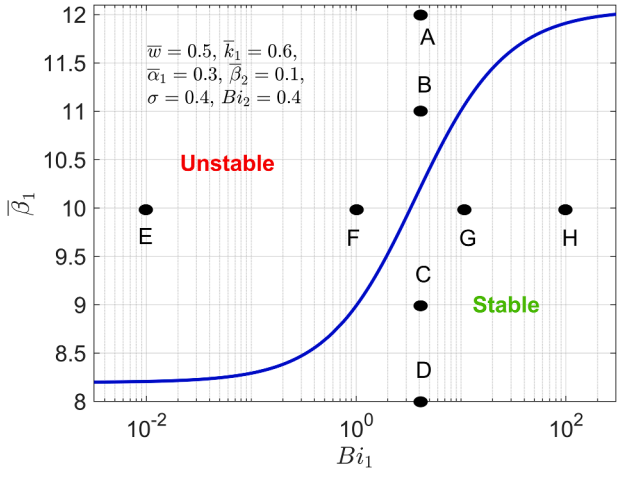

Fig. 8. Stable and unstable regions in the design space: Plot of maximum possible $\bar{\beta}_1$ to ensure thermal stability as a function of Bi_1. Other problem parameters are $\bar{k}_1 = 0.6,\ \bar{\alpha}_1 = 0.3,\ \bar{\beta}_2 = 0.1,\ \bar{w} = 0.5,\ \sigma = 0.4, Bi_2 = 0.4$. Stable and unstable regions are indicated. Eight design points are indicated for further illustration.

In general, heat removal from the two ends of the layered body is also important, but since this has been studied in detail in the past [2,10], therefore, this is not considered explicitly in the present work, and the top/bottom boundaries are assumed to be isothermal.

In order to identify and illustrate converging and diverging regions in the design space of the two-layer body comprising the non-dimensional parameters listed above, pole analysis is used to determine stability of the body over the $\bar{\beta}_1$-Bi_1 space while holding all other parameters constant. For each boundary dissipation condition, represented by Bi_1, the maximum tolerable heat generation characteristic represented by $\bar{\beta}_1$ in order to ensure stability is computed. In this manner, a stability curve is generated and presented in Fig. 8. Other problem parameters are $\bar{k}_1 = 0.6;\ \bar{\alpha}_1 = 0.3;\ \sigma = 0.4;\ Bi_2 = 0.4;\ \bar{w} = 0.5,\ \bar{\beta}_2 = 0.1$. Fig. 8 plots the threshold curve below and to the right of which, the body is thermally stable, and above and to the left of which, the body is thermally unstable. In general, Fig. 8 shows that the larger the value of Bi_1, the larger is the amount of temperature-dependent heat generation that the body can tolerate while remaining within the stable regime. Note that very small and very large values of Bi_1 correspond to adiabatic and isothermal conditions, respectively, which are the worst-case and best-case conditions for stability, respectively. The stability curve is found to be S-shaped, indicating that when conditions at the boundary are very adverse (small Bi_1), small improvements in cooling conditions do not result in significant benefit in terms of how much heat the body can withstand. At the other end of the curve, when Bi_1 is already quite large, therefore approaching isothermal conditions, incremental improvement in Bi_1 does not bring about significantly increased heat removal. These arguments explain the flat nature of the curve in Fig. 8 at the two ends. In between the two ends, there is a steep region in which the threshold value of $\bar{\beta}_1$ improves rapidly with increasing Bi_1. From a design perspective, this implies it may be desirable to improve boundary conditions when operating in this steep intermediate region, whereas, if Bi_1 is relatively small or large, efforts to increase Bi_1 may not be justified due to the limited incremental thermal benefit from doing so.

The converging and diverging regions identified in Fig. 8 may be of much practical importance. For example, points A, B, E and F shown in Fig. 8 are thermally unstable, while points C, D, G and H are stable. Points A, B, C and D represent multiple heat generation conditions (i.e., $\bar{\beta}_1$) at a constant Bi_1, whereas points E, F, G and H represent multiple boundary cooling conditions (i.e., Bi_1) at constant $\bar{\beta}_1$. In order to further illustrate the impact of changing $\bar{\beta}_1$ or Bi_1 on thermal stability, temperature at a specific location in the body is plotted as a function of time for these design points. The temperature field is computed by inverse Laplace transformation of the solution derived in the Laplace domain. The case of multiple $\bar{\beta}_1$ at constant Bi_1 is presented in Fig. 9(a). Consistent with the stable and unstable regions shown in Fig. 8, the temperature curves in Fig. 9(a) show thermal instability for points D ($\bar{\beta}_1 = 8$) and C ($\bar{\beta}_1 = 9$), whereas increasing $\bar{\beta}_1$ further results in crossing the stability curve into the unstable region, so that the points B ($\bar{\beta}_1 = 11$) and A ($\bar{\beta}_1 = 12$) are unstable.

Similar illustration of the impact of increasing Bi_1 at constant $\bar{\beta}_1$ is presented in temperature plots for points E, F, G and H in Fig. 9(b). As expected, it is found that the problem is thermally stable when Bi_1 is sufficiently large, for example at points G ($Bi_1 = 10$) and H ($Bi_1 = 100$), whereas reducing Bi_1 results in instability, for example at points E ($Bi_1 = 0.01$) and F ($Bi_1 = 1$).

5.7. Effect of thermal diffusivity

In addition to heat generation and boundary dissipation processes investigated in previous sub-sections, diffusion within layers is also an important process that governs whether the problem is thermally stable or not. The thermal diffusivity $\bar{\alpha}_1$ is the key thermal property that governs this process. In general, it is expected that a larger thermal diffusivity would contribute towards greater removal of heat, and, therefore,

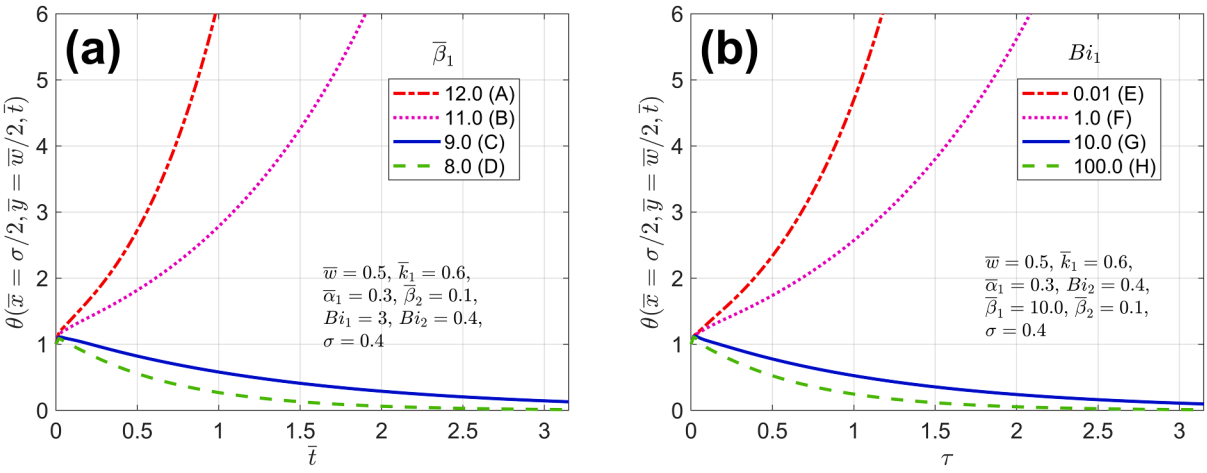

Fig. 9. Illustration of thermal stability as a function of reaction term and boundary condition: Temperature at $\bar{x} = \sigma/2,\ \bar{y} = \bar{w}/2$ as a function of time for different values of (a) $\bar{\beta}_1$ (with $Bi_1 = 3$) and (b) Bi_1 (with $\bar{\beta}_1 = 10$), respectively. Other problem parameters are $\bar{k}_1 = 0.6,\ \bar{\alpha}_1 = 0.3,\ \bar{\beta}_2 = 0.1,\ \bar{w} = 0.5,\ \sigma = 0.4,\ Bi_2 = 0.4$.

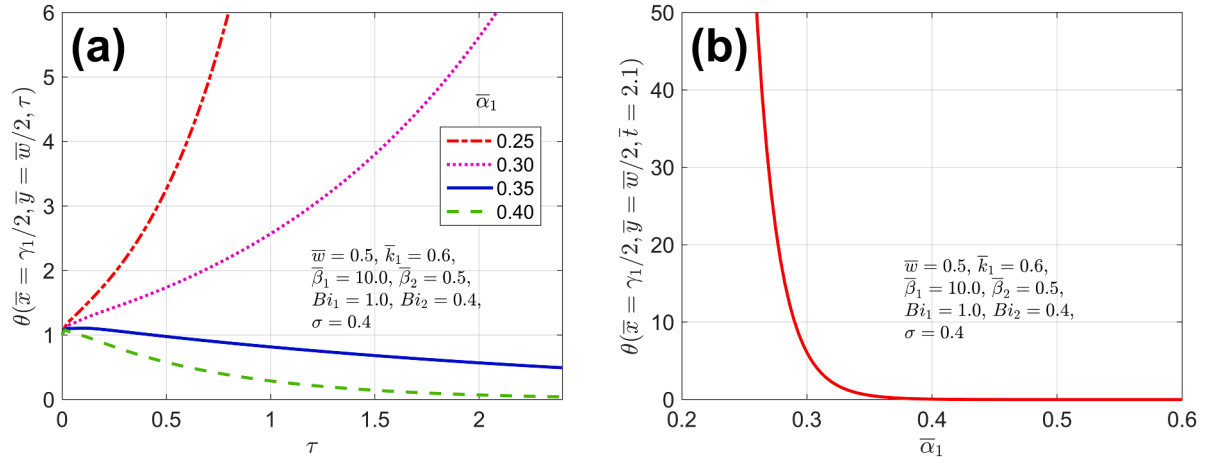

Fig. 10. Effect of thermal diffusivity on stability: (a) Temperature vs time curves for multiple values of $\bar{\alpha}_1$, (b) Temperature at a large time as a function of $\bar{\alpha}_1$. Other problem parameters are $\bar{k}_1 = 0.6,\ \sigma = 0.4,\ \bar{\beta}_1 = 10.0,\ \bar{\beta}_2 = 0.5,\ Bi_1 = 1,\ Bi_2 = 0.4,\ \bar{w} = 0.5$.

thermal stability. In order to illustrate this quantitatively, temperature vs time plots are presented in Fig. 10(a) for a representative problem with different values of $\bar{\alpha}_1$. Similar to previous Figures, the temperature field is computed by inverse Laplace transformation of the solution derived in the Laplace domain. As expected, it is found that relatively smaller values of $\bar{\alpha}_1$ lead to thermal instability and large temperature rise at large times, whereas the temperature plot decays over time when $\bar{\alpha}_1$ is sufficiently large. In fact, thermal stability of this problem is strongly dependent on $\bar{\alpha}_1$, with relatively minor changes in $\bar{\alpha}_1$ resulting in sharp transition from stable to unstable configuration. To illustrate this, temperature at a large time, $\bar{t} = 2.1$ is plotted as a function of $\bar{\alpha}_1$ in Fig. 10(b). This plots shows that the temperature decays to zero for sufficiently large values of $\bar{\alpha}_1$ and that there is a very sharp transition from stable to unstable configuration as $\bar{\alpha}_1$ is reduced. Close to around $\bar{\alpha}_1 = 0.3$, even a small improvement in $\bar{\alpha}_1$ may shift the thermal behavior of the system from unstable to stable. This may have important practical implications in the design of thermal systems. In case the thermal diffusivity of a system is close to such a threshold as illustrated in Fig. 10 (b), then even minor improvement in $\bar{\alpha}_1$, which may be easy to accomplish through, for example, material changes or introduction of additives, may ensure the thermal stability of the system. In contrast, even minor reduction in thermal diffusivity, for example, due to material deterioration or aging may cause the system to fall into a thermally unstable regime.

5.8. Extension to non-isothermal boundary conditions along the layered direction

As shown in Eqs. (15) and (16), the analysis presented here assumes isothermal conditions at the two boundaries along the layered direction, at $\bar{x} = 0,\ 1$. This assumption has been made to simplify the analysis and focus on boundary conditions induced by the two-dimensionality of the problem. This is a reasonable approach since the influence of boundary conditions $\bar{x} = 0,\ 1$ on thermal stability of multilayer diffusion-reaction problems has been analyzed extensively in past work [2,10]. In contrast to such past work, the assumption of isothermal boundary conditions at $\bar{x} = 0,\ 1$ in the present work facilitates emphasis on sidewall boundary conditions in the direction normal to the layers.

While isothermal boundary condition at $\bar{x} = 0,\ 1$ is a reasonable model for some practical conditions, such as when the multilayer stack is sandwiched between isothermal cold plates, or is being cooled by a boiling coolant, nevertheless, extension of the theory presented here to non-isothermal conditions is quite straightforward and may be helpful for other practical problems. In brief, the coefficients $C_{1,n}$ and $C_{2,n}$, which are given explicitly by Eq. (37) for the isothermal case are no longer available explicitly when the boundary condition is replaced by a

more general convective condition. Instead, $C_{1,n}$ and $C_{2,n}$ are now coupled to $D_{1,n}$ and $D_{2,n}$ through linear algebraic equations arising from the convective boundary conditions at $\bar{x} = 0,\ 1$. In such a case, the set of algebraic equations needs to be expanded to include $C_{1,n}$ and $C_{2,n}$ in addition to $D_{1,n}$ and $D_{2,n}$. The determinants associated with this expanded set of equations continue to predict the thermal stability of the system in a manner similar to the discussion in Section 4.

6. Conclusions

The key novelty of the present work is that it accounts for two-dimensional heat transfer in determining the thermal stability of multilayer diffusion-reaction problems. This work improves upon past work in which thermal stability analysis was limited only to one-dimensional geometry. Problems that may benefit from the present analysis occur commonly in practical systems such as Li-ion cells and other reacting systems, where the two-dimensional nature of the geometry must be accounted for. This work shows that the thermal stability of such a problem can be analyzed through the relatively simple calculation of the various determinants associated with a set of algebraic equations.

While this work is presented in the context of a two-layer body, extension to more than two layers is conceptually straightforward. The number of unknown coefficients will be greater in such a case, but, nevertheless, a sufficient set of linear algebraic equations can continue to be written based on conditions at each interface. Another key assumption made in this work is the linearization of temperature-dependent heat generation. Such linearization is commonly carried out as an approximation [2,10,17], since it enables the use of mathematical tools such as separation of variables [2,10,11] and linear stability analysis [17]. However, for any given problem, the appropriateness of such linearization must always be examined before the use of analytical tools developed in this work. Other key assumptions behind this work include temperature-independent thermal properties and uniform convective heat transfer coefficient over each layer.

While this work primarily contributes towards the theoretical understanding of thermal stability, the results presented here may also be used for design and optimization of practical engineering systems. Diffusion-reaction in multilayer geometry occurs commonly, for example, in Li-ion cells and other reacting systems. Accounting for two-dimensional heat flow may be important in such cases. The key results presented here may be useful for predicting whether a particular system with given properties and other characteristics is stable or not, and to design systems that offer thermal safety.

CRediT authorship contribution statement

Ankur: Conceptualization, Methodology, Formal analysis, Investigation, Data curation, Visualization, Supervision, Project administration, Writing – original draft, Writing – review & editing. **Girish Krishnan:** Conceptualization, Formal analysis, Investigation, Data curation, Visualization, Writing – original draft, Writing – review & editing.

Declaration of Competing Interest

The authors declare that they have no known competing financial interests or personal relationships that could have appeared to influence the work reported in this paper.

Data availability

Data will be made available on request.

References

[1] A. Kolmogorov, I. Petrovskii, N. Piskunov, Study of a diffusion equation that is related to the growth of a quality of matter and its application to a biological problem, Mosc. Univ. Math. Bull. 1 (1937) 1–26.

[2] A. Jain, M. Parhizi, L. Zhou, G. Krishnan, Imaginary eigenvalues in multilayer one-dimensional thermal conduction problem with linear temperature-dependent heat generation, Int. J. Heat Mass Transf. 170 (2021), 120993, https://doi.org/10.1016/j.ijheatmasstransfer.2021.120993, 1-10.

[3] B. Yang, H. Shi, A thermal stability criterion for heat conduction in multilayer composite solids, J. Heat Transf. 131 (2009) 11304, https://doi.org/10.1115/1.3153581, 1-7.

[4] A. Jain, S. McGinty, G. Pontrelli, L. Zhou, Theoretical model for diffusion-reaction based drug delivery from a multilayer spherical capsule, Int. J. Heat Mass Transf. 183 (2022), 122072, https://doi.org/10.1016/j.ijheatmasstransfer.2021.122072, 1-14.

[5] D. Arifin, L.Y. Lee, C.H. Wang, Mathematical modeling and simulation of drug release from microspheres: implications to drug delivery systems, Adv. Drug Deliv. Rev. 58 (2006) 1274–1325, https://doi.org/10.1016/j.addr.2006.09.007.

[6] Y.B. Zeldovich, D.A. Frank-Kamenetskii, A theory of thermal flame propagation, Acta Phys. Chim. Sin. 9 (1938) 341. USSR.

[7] J.R. Lamarsh, Introduction to Nuclear Engineering, Addison-Wesley, Reading, MA, 1975.

[8] R.S. Cantrell, C. Cosner, Spatial Ecology via Reaction-Diffusion Equations, 1st Ed., ISBN, Wiley, 2003, pp. 978–0471493013.

[9] B. Hobbs, A. Ord, 'Nonlinear dynamics,' In: 'Structural Geology,' B. Hobbs, A. Ord, pp. 189–240, 2015. DOI: 10.1016/B978-0-12-407820-8.00007-2.

[10] G. Krishnan, A. Jain, Derivation of multiple but finite number of imaginary eigenvalues for a two-layer diffusion-reaction problem, Int. J. Heat Mass Transf. 194 (2022), 123037, https://doi.org/10.1016/j.ijheatmasstransfer.2022.123037, 1-7.

[11] K. Shah, D. Chalise, A. Jain, Experimental and theoretical analysis of a method to predict thermal runaway in Li-ion cells, J. Power Sources 330 (2016) 167–174, https://doi.org/10.1016/j.jpowsour.2016.08.133.

[12] T.M. Bandhauer, S. Garimella, T.F. Fuller, A critical review of thermal issues in lithium-ion batteries, J. Electrochem. Soc. 158 (2011) R1–R25, https://doi.org/10.1149/1.3515880.

[13] D. Mishra, A. Jain, Multi-mode heat transfer simulations of the onset and propagation of thermal runaway in a pack of cylindrical li-ion cells, J. Electrochem. Soc. 168 (2021), 020504, https://doi.org/10.1149/1945-7111/abdc7b, 1-11.

[14] G. Krishnan, A. Jain, Theoretical analysis of a two-dimensional multilayer diffusion problem with general convective boundary conditions normal to the layered direction, Int. J. Heat Mass Transf. 202 (2023), 123723, https://doi.org/10.1016/j.ijheatmasstransfer.2022.123723.

[15] G. Krishnan, A. Jain, Diffusion and reaction in a two-dimensional multilayer body: analytical solution and imaginary eigenvalue analysis, Int. J. Heat Mass Transf. 196 (2022), 123163, https://doi.org/10.1016/j.ijheatmasstransfer.2022.123163, 1-11.

[16] K.L. Hitz, T.E. Fortmann, An Introduction to Control Systems, CRC Press, 1977. ISBN: 978-0824765125.

[17] A. Jain, Analysis of a diffusion-reaction heat transfer problem in a finite thickness layer adjoined by a semi-infinite medium, Int. J. Heat Mass Transf. 205 (11) (2023), 123919, https://doi.org/10.1016/j.ijheatmasstransfer.2023.123919.

[18] A. Haji-Sheikh, J. Beck, Temperature solution in multi-dimensional multi-layer bodies, Int. J. Heat Mass Transf. 45 (2002) 1865–1877, https://doi.org/10.1016/S0017-9310(01)00279-4.

[19] F. de Monte, Unsteady heat conduction in two-dimensional two slab-shaped regions. Exact closed-form solution and results, Int. J. Heat Mass Transf. 46 (2003) 1455–1469, https://doi.org/10.1016/S0017-9310(02)00417-9.

[20] H. Salt, Transient conduction in a two-dimensional composite slab—II. Physical interpretation of temperature modes, Int. J. Heat Mass Transf. 26 (1983) 1617–1623, https://doi.org/10.1016/S0017-9310(83)80081-7.

[21] M.D. Mikhailov, M.N. Özişik, Transient conduction in a three-dimensional composite slab, Int. J. Heat Mass Transf. 29 (1986) 340–342, https://doi.org/10.1016/0017-9310(86)90242-5.

[22] R. Spotnitz, J. Franklin, Abuse behavior of high-power, lithium-ion cells, J. Power Sources 113 (2003) 81–100, https://doi.org/10.1016/S0378-7753(02)00488-3.

[23] F.R. de Hoog, J.H. Knight, A.N. Stokes, An improved method for numerical inversion of Laplace transforms, SIAM J. Sci. Stat. Comput. 3 (1982) 357–366.

[24] K.J. Hollenbeck, 'INVLAP.M: a matlab function for numerical inversion of laplace transforms by the de Hoog algorithm,' available at http://www.isva.dtu.dk/staff/karl/invlap.htm, accessed 1/1/2012.

[25] G. Strang, Linear Algebra and Its Applications, 4th Ed., Wellesley-Cambridge Press, 2009.